



FUNCTIONALIZATION OF *PARKIA BIGLOBOSA* MEDIATED-GOLD NANOPARTICLE FOR IMPROVED DRUG DELIVERY

*¹Okoampah, E., ²Dauids, J. S., ²Payne, J.

¹Department of Biochemistry and Molecular Biology, Faculty of Biosciences, University for Development Studies, P.O. Box TL1882, Tamale, Ghana.

²Department of Biotechnology, Faculty of Biosciences, University for Development Studies, P.O. Box TL1882, Tamale, Ghana.

*Corresponding Author's: Email: jdauids@uds.edu.gh

Abstract

NPs have emerged as promising in the pharmaceutical industry, prompting several studies into their potential as drug delivery agents due to their biocompatibility with cellular structures. Antibiotic resistance has increased over time, as has the unrealistic bio-distribution of antibiotics to disease sites, making it critical to improve antibiotic efficiency in order to cure disease. This study investigated the bio-reduction and stability potential of H₂AuCl₄ by obtaining gold nanoparticles (AuNPs) from the leaves of *Parkia biglobosa* and studying their drug release potential using three nanodrug composites, PD (PEG conjugated on lincomycin), PN (PEG conjugated on AuNPs), and PND (PEG conjugated on AuNPs) (PEG and lincomycin on AuNPs). UV-Vis spectrophotometry, TEM, FTIR, XRD, and EDS were used to characterize the as-synthesized AuNPs and the formulated nanodrug composites. For all three drug composites, an optimal released capacity was reached at 9 minutes after an initial drug release capacity at 3 minutes for PD, PN, and PND. PND had a release capacity of 23mg/ml, followed by PD and PN with 12mg/ml and 4.8mg/ml, respectively. The high drug release capacity observed in the PND composite was due to the AuNPs' biocompatibility and the ability of PEG to prevent degradation. The antimicrobial activity of the formulated drug composites were able to inhibit the growth of the microbes with PND inhibiting the growth of *Pseudomonas aeruginosa*, *Enterococcus faecalis*, *Staphylococcus aureus*, and *Escherichia coli* at 43.25mm, 20.25mm, 33.00mm, and 28.00, respectively; followed by PD with the zones of inhibition at 41.75mm, 19.00mm, 30.75mm, and 23.50mm, respectively. PND and PN both inhibited *Candida albicans* with zones of inhibition of 50.31mm and 49.34mm, respectively. Interestingly, PN had no zone of inhibition on the microbes or fungi. The combined drug release potential and microbial growth inhibition of the as-synthesized formulated drugs provides a new generation technology to improve disease treatment capacity of pharmaceutical drugs.

Keywords: Gold Nanoparticles; Antibiotics; Drug Release; Microbes; Polymer

Introduction

Metallic nanoparticles (NPs) have emerged as a research topic in the development of site-specific agents based on copper, silver, gold nanoparticles, and many others as nano-drug carriers for disease target delivery of therapeutic agents. AuNPs have piqued the interest of biomedical researchers due to their inherent physicochemical properties such as biocompatibility, surface chemistry, easily tunable size and shape, and easy surface functionalization due to AuNPs stable thiol chemistry (Okoampah et al., 2020; Zhang et al., 2010). For example, the functionalization of AuNPs with doxycycline served as a nano-drug carrier for doxorubicin, an anti-cancer drug, which was then delivered to the cancer site (Singh et al., 2017; Kazmi et al., 2019). The rise in microbial resistance and unrealistic bio-distribution of existing antibiotics has be-

come a public health concern, necessitating the development of new antibiotics or improving the efficacy of existing ones. Due to their extensive exploration in medical research, particularly as a nano-drug carrier for disease site targeted drug delivery, the market for nanotechnology that enhances the uses of AuNPs as one of the fundamental units of nanotechnology is worthy of curbing the growing menace of antibiotic inefficiencies (Okoampah et al., 2020; Shittu et al., 2017). Interestingly, AuNPs have a medical application because they can be functionalized with polymers, dendrimers, proteins, and other molecules to avoid serum protein adsorption and have a longer blood circulation time to successfully target a site of interest. It is worth noting that polyethylene glycol (PEG), a popular polymer, has been used as a capping agent for AuNPs in order to prevent degrada-

tion prior to delivery while also providing immune system compatibility such as non-immunogenicity, non-antigenicity, and protein serum adsorption. (Del Pino et al., 2016; Lin, 2016). Because AuNPs capped with PEG, they are not recognized as foreign and thus cannot be cleared from the body, they are an ideal candidate for efficient drug delivery and bio-distribution to disease sites (Chen et al., 2013).

The synthesis of AuNPs is important, as the chemical and physical synthesis approaches have been used to obtain AuNPs from their bulk metals. However, recent literature has revealed that the popular chemical and physical AuNPs synthesis approaches are not environmentally friendly due to toxicity (Agarwal et al., 2017; Bhardwaj et al., 2020). Against this background, the biological AuNPs synthesis approach has emerged as an alternative, as it has been reported to be environmentally friendly with zero toxicity and to be simple to use in AuNPs synthesis (Kaur & Sidhu, 2021). For example, the bio-reduction of chloroauric acid (HAuCl₄) for the synthesis of AuNPs with *Hygrophila spinosa* aqueous leaf extract has been reported to be non-toxic which were able to inhibit the growth of clinically isolated human pathogens (Koperuncholan, 2015).

The researchers previously investigated the antimicrobial potential of *Parkia biglobosa* leaves mediated-AuNPs, which were capable of inhibiting the growth of *Staphylococcus aureus*, *Enterococcus faecalis*, *Escherichia coli*, and *Pseudomonas aeruginosa* (Davids, 2020). To address the bottlenecks of antibiotic resistance and unrealistic antibiotic drug biodistribution, we modified our biosynthesized AuNPs by capping them with PEG, which has the potential to prevent serum protein adsorption and give our AuNPs a longer residence time in order to achieve successful site targeting. We studied the drug release efficiency and antimicrobial activity of the formulated nano-drug, PD (PEG conjugated on lincomycin), PN (PEG conjugated on AuNPs), and PND (PEG and lincomycin conjugated on AuNPs) against some selected clinical microbes, including *Staphylococcus aureus*, *Escherichia coli*, *Enterococcus faecalis*, *Pseudomonas aeruginosa*, and *Candida albicans*. Findings from this study will enhance the quest of making biosynthesized AuNPs a new generation nanomaterial functioning as antibiotics and nano-drug carrier agents.

Materials and Methods

Reagent

All reagents used were analytical pure and do not require further purification before use. Hydrogen tetra auric acid (HAuCl₄) and polyethylene glycol (MW3000) were obtained from Sigma Aldrich Company, USA. Antibiotic

lincomycin was also gotten from Sigma Aldrich company. Mueller Hinton agar, nutrient broth, Deionized water, ethanol, methanol.

Plant Material

Parkia biglobosa leaves were obtained from the University for Development Studies, Tamale in the Northern Region of Ghana.

Microbes

The microorganisms used were *Staphylococcus aureus*, (ATCC 29213) *Escherichia coli*, (ATCC 25922) *Pseudomonas aeruginosa* (ATCC 27853), *Enterococcus faecalis* (ATCC 29212) and *Candida albicans* (CMCC98001).

Extraction Procedure

The extraction was carried out in accordance with the procedure outlined in our previous studies (Davids, 2020). The *Parkia biglobosa* leaves were thoroughly washed with distilled water before drying for one hour at 95 °C. The leaves were then ground into a fine powder. Following that, 5 g of the plant sample (*Parkia biglobosa*) was weighed and dissolved in 100 ml of sterile distilled water in an Erlenmeyer flask. The solution was then filtered using Whatman's no. 1 filter paper to obtain clearer extracts. Following Akinyemi et al. (2005) and Davids et al. (2021). The obtained extracts were stored for further qualitative phytochemical screening for major constituents.

Preliminary Phytochemical Analysis

Test for flavonoids: 1 mL of aqueous extract was mixed with 1 mL of a 10% lead acetate solution. The presence of a yellow precipitate was considered a positive test for flavonoids.

Test for Alkaloids: On a steam bath, 3 mL of aqueous extract was mixed with 3 mL of 1 percent HCl. The mixture was then treated with Mayer's and Wagner's reagents. The presence of alkaloids was determined by the turbidity of the resulting precipitate.

Test for tannins: 2 mL of the aqueous extract was mixed with 2 mL of distilled water, followed by a few drops of FeCl₃ solution. The presence of tannins was indicated by the formation of a green precipitate.

Test for saponins: In a test tube, 5 mL of aqueous extract was vigorously shaken with 5 mL of distilled water and warmed to 100°C. The presence of saponins was determined by the formation of stable foam.

Test for terpenoids: 2 mL of the organic extract was dissolved in 2 mL of chloroform and dried. After that, 2 mL of concentrated sulphuric acid was added and heated for about 2 minutes. Terpenoids are present when the



Fig. 1: *Parkia Biglobosa* (Dawadawa) Plant

color is greyish.

Tests for steroids: 2 mL of ethanol extract was dissolved in 2 mL of chloroform, followed by 2 mL of concentrated sulphuric acid. The presence of steroids was indicated by the formation of a red color in the lower chloroform layer. Tests for carbohydrates: 1 mL of iodine solution was added to 3 mL of aqueous extract. The presence of carbohydrate is indicated by a purple coloration at the interphase. Tests for glycosides: Following Salkowski's test, 2 mL of aqueous extract were briefly dissolved in 2 mL of chloroform. 2 mL of sulphuric acid was carefully added and gently shaken. A steroidal ring is indicated by a reddish brown color (that is a glycone portion of glycoside).

Tests for anthraquinones: Following Borntrager's test, 3 mL of aqueous extract was briefly shaken with 3 mL of benzene, filtered, and 5 mL of 10% ammonia solution was added to the filtrate. After shaking the mixture, the presence of a pink, red, or violet color in the ammoniacal (lower) phase indicates the presence of free anthraquinones.

Biosynthesis of *Parkia Biglobosa* Mediated- Gold Nanoparticles

The biosynthesis of the approach was carried out in accordance with the procedure outlined by Alaa et al. (2013), with minor modifications. In a nutshell, 5 g of the plant

sample (*Parkia biglobosa*) was weighed and mixed with 100 ml of sterile distilled water in an Erlenmeyer flask for 5 minutes before being filtered. Following that, 5 mL of plant extract was added to 45 mL of 1 mM aqueous HAuCl₄ solution under magnetic stirring at room temperature. A reddish-brown color was observed, indicating that the AuNPs were successfully synthesized.

Purification of *Parkia Biglobosa* Mediated Gold Nanoparticles

The purification procedure was followed with minor modifications as described by Alaa et al. (2013). To remove any large aggregates, the as-biosynthesized AuNPs were centrifuged at 14,000 RPM (benchtop, Eppendorf, Thermo Fisher Scientific, Darmstadt, Germany) for 20 minutes and repeated 6 times. The supernatant was collected and purified further by dialyzing against 10 mM deionized water with 20 kDa dialysis bags (Spectrum Labs) at 2 h intervals twice, followed by overnight incubation for 15-18 h.

Characterization of Biosynthesized *Parkia Biglobosa* Mediated Gold Nanoparticles

The transmission electron microscope (TEM) was used on a JEOL model 1200EX instrument, and a few drops of AuNPs were deposited on Lacey carbon grids with a mesh of 300. (SPI supplies, 3330C-CF). It was air-dried and photographed. It was subjected to an accelerating voltage of 80 kV in order to determine its morphology, which included shape, size, and purity. To assess the functional groups of the AuNPs, the elemental composition was analyzed using energy-dispersive X-ray spectroscopy (EDS) S-3400 N and Fourier transform infrared spectroscopy (FTIR). A UV-1800 Shimadzu spectrophotometer was used to measure the UV-spectroscopy of the HAuCl₄-plant extract solution. The X-ray diffraction spectrum was used to examine the crystallinity. The various peaks in the mixture were then measured over a wavelength range of 230-1000 nm (Davids, 2020).

Functionalization of Biosynthesized AuNPs

The AuNPs were functionalized in the manner described by Shittu et al. (2017) with minor modifications. In brief, the functionalization of AuNPs was investigated using a conventional medicine (lincomycin) and polyethylene glycol (Shittu et al., 2017). The formulations were designed to produce three distinct composites from three separate components. The first formulation (polyethylene glycol, gold nanoparticles, and drug (PND) was made by combining 0.5 ml of biosynthesized AuNPs with 5 g of polyethylene glycol and 0.58 g of lincomycin

and stirring for 1 hour with a magnetic stirrer. The second formulation (polyethylene glycol and gold nanoparticles (PN) composite) was made by adding 0.5 ml of biosynthesized AuNPs to 5 g polyethylene glycol and stirring for 1 hr. The third formulation (composite of polyethylene glycol and drug (PD)) was made by blending 1 ml of sterile deionized water with 0.58 g of conventional drug and 5 g of polyethylene glycol for 1 hour. All of the designs were frozen for 2 hours before being made into tablets by freeze-drying for 24 hours. The samples were then placed in an incubator for 24 hours at 37 °C to allow wet digestion of the mixture before being properly air-dried.

- PD = PEG+ Drug. (1)
 PN = PEG + AuNPs (2)
 PND = PEG + AuNPs + Drug Shittu et al. (2017) (3)

Drug Release

The drug release was carried out in a sterile environment, as described by Shittu et al. (2017). The drug was released in a clean environment using test tubes containing 3 mL of sterile deionized water for each formulation. The height and diameter of each tablet were measured before immersing it in 3 ml of sterile deionized water for 3 minutes, after which the height and diameter were measured again, and the process was repeated until the entire tablet was dissolved, and the normal medication concentration and absorption of the various formulations were analyzed using a UV-Vis spectrophotometer.

Anti-Microbial Efficiency

Antibacterial Assay

Muller 9.5g In 250 mL of sterile distilled water and 10 cm³ of nutrient broth, Hinton agar was dissolved. To grow these pathogenic bacteria, the broth culture was used in an antibacterial assay. After that, it was autoclaved for 15 minutes at 121°C. In the same manner, the deionized water used in drug discharge was sterilized. After sterilization, the samples were allowed to cool to about 45 °C before the nutrient agar was distributed into Petri dishes to solidify. The formulated substances (PD, PN, and PND) were then impregnated into a paper disk with a diameter of 10 mm, and the cultures were swabbed on test media with a sterile cotton swab. To create a confluent lawn of bacterial growth, approximately the same amount of bacterial cultures from all strains were spread across the Petri plate. Inoculated drugs were roughly designed, and the plates were incubated at 37 °C for 24 hours. Following incubation, the diameter of the inhibition area (mm) was measured.

Antifungal Assay Protocols for Preparing Potatoes Dextrose Agar Media

Peeled potatoes weighing 200 g were made into chips. The sliced potatoes were cooked in a pan with 1000 ml of water for 20 minutes. In a clear beaker, glucose and agar were tested. A graduated cylinder covered with gauze was used to filter the boiled potatoes. The infusion was then introduced overnight to the graduated cylinder containing glucose and agar, as well as the frozen culture medium.

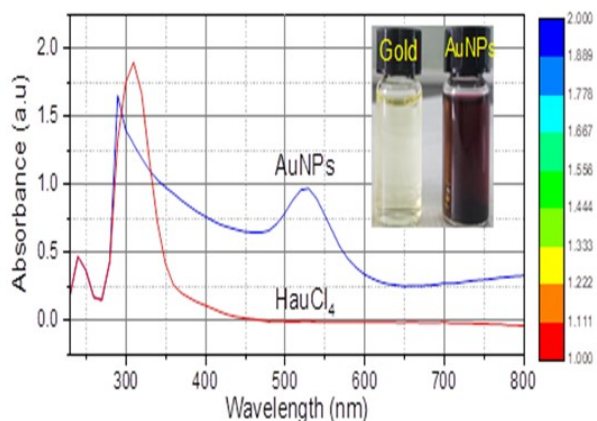
Anti-Fungi Activities

Candida albicans cells were suspended at PH 7.4 in 20 mM sodium phosphate buffer, then mixed in water with 20 microliters of formulated drugs at 5 g/mL and incubated at 37 °C for 2 hours with shaking at 550 rpm. The reaction was then diluted to PH 7 by adding 5 mM of 360mL phosphate buffer. Cells were then spread on PDA and incubated for 24 hours at 37 °C. The loss of viability has been calculated as

$$\frac{1 - \text{colony-forming units CFUs in the presence of AuNPs}}{\text{Colony-forming units without AuNPs}} \times 100$$

Results

a



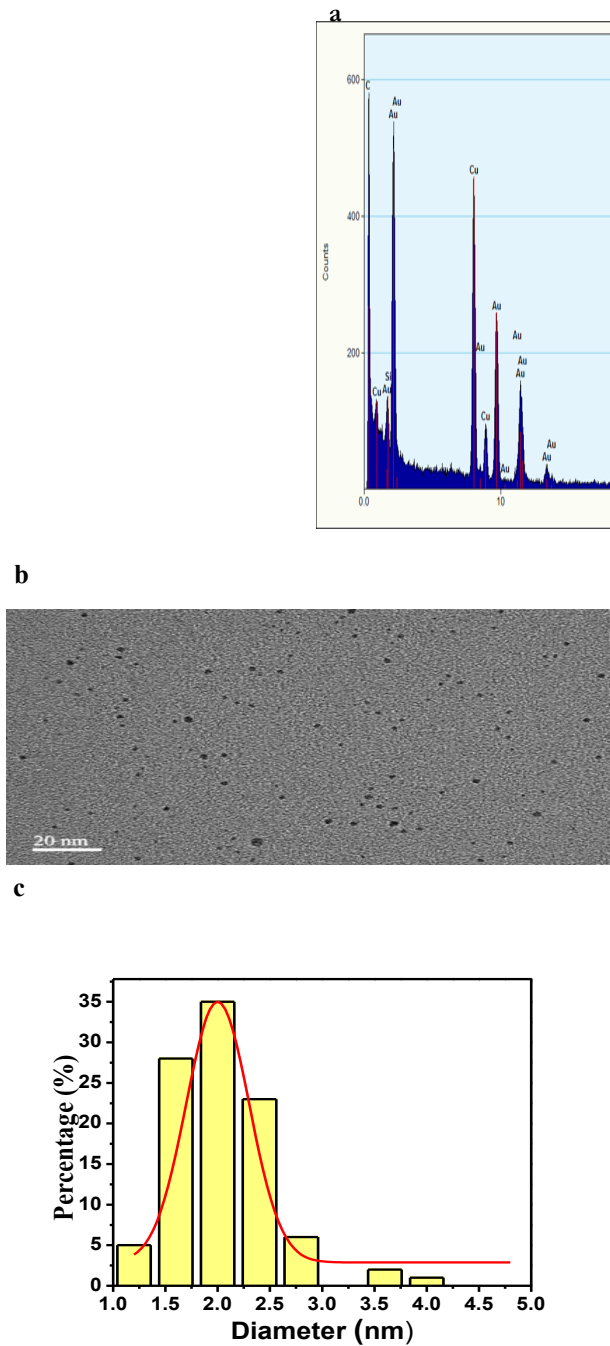


Figure 2: Schematic representation of: (a) UV-Vis absorption spectra of H₂AuCl₄ and *Parkia biglobosa* mediated AuNPs; (b) TEM image of *Parkia biglobosa* mediated AuNPs; and (c) Size distribution based on the TEM images of *Parkia biglobosa* mediated AuNPs

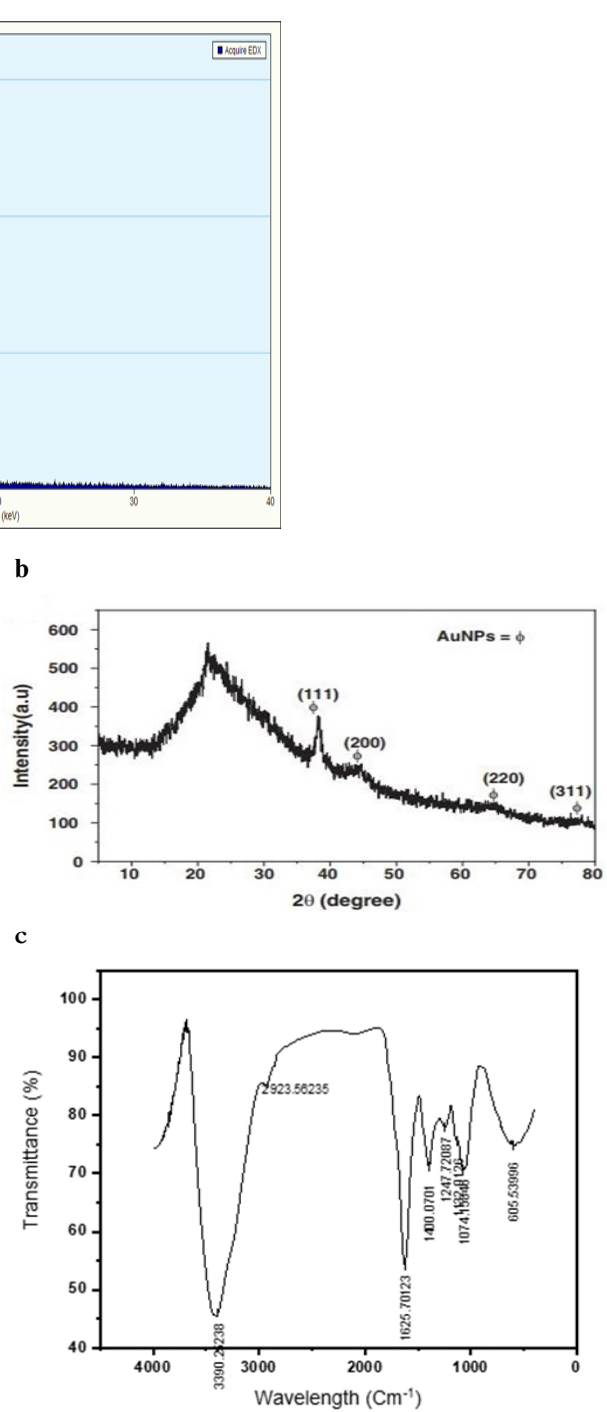


Figure 3: (a) Electron Diffraction Spectroscopy; (b) X-ray diffraction spectrum; (c) Fourier transmission Infrared (FTIR) image of *Parkia biglobosa* mediated AuNPs

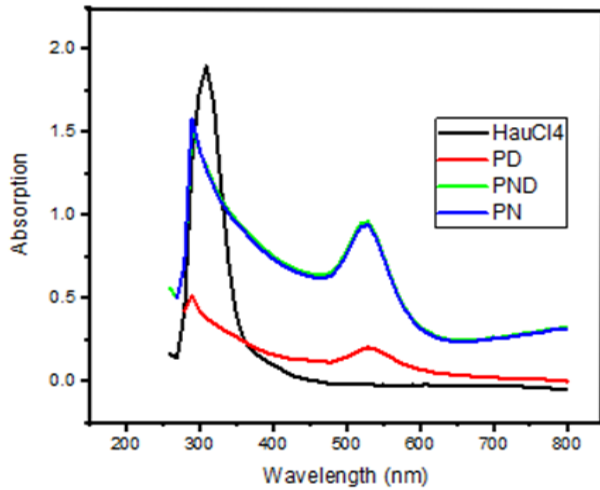


Figure 4 (a) UV-Vis absorption spectrum of formulated nanodrugs (PD, PND, PN, and HAuCl4)

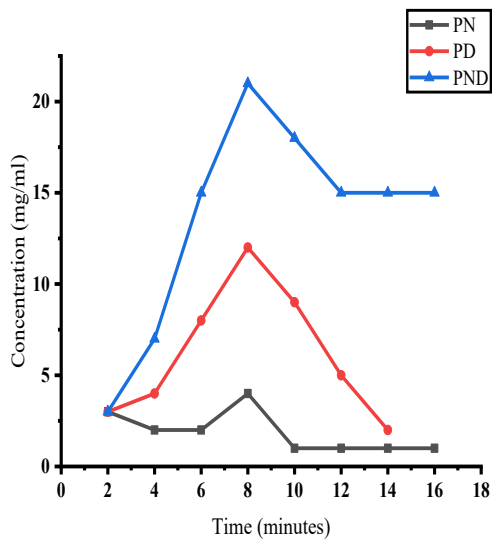


Figure 4 (b) Drug release efficiency of the 3 nanodrug composites (PD, PND, and PN)

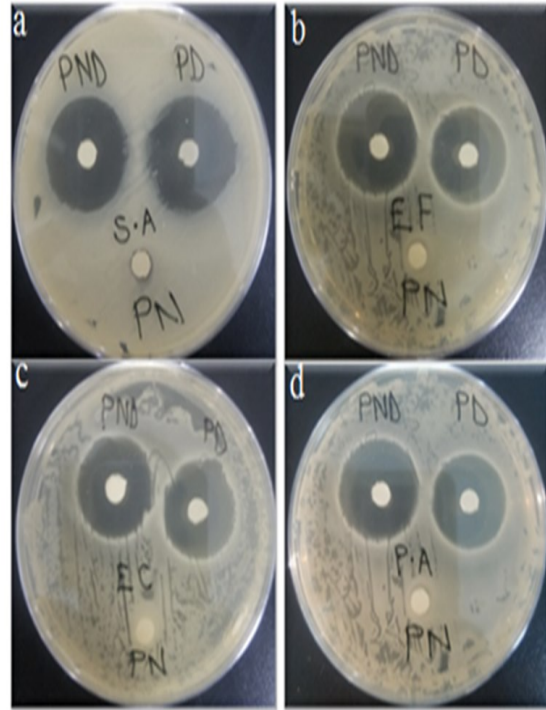


Figure 5: Anti-bacterial efficacy of the formulated drugs a) on *Staphylococcus aureus* b) *Enterococcus faecalis* c) *Escherichia coli* d) *Pseudomonas aeruginosa*

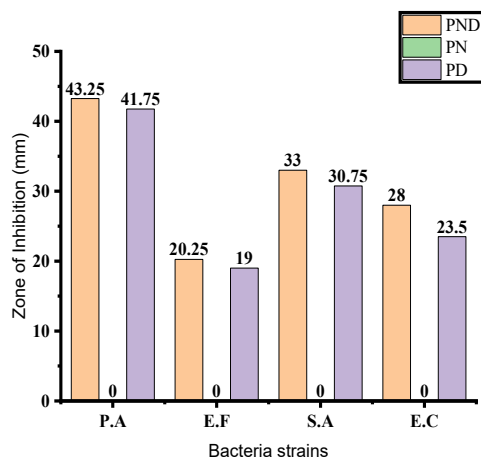


Figure 6: A graphic representation of anti-bacterial zone of inhibition of the various drugs against the four (4) bacterial strains where *Pseudomonas aeruginosa* is represented as P.A

DISCUSSION

Biosynthesis and Characterization

Preliminary qualitative phytochemical analysis of *Parkia biglobosa* leaves revealed the presence of alkaloids, tannins, cardiac glycosides, flavonoids, saponins, amino acids, and steroids. As previously demonstrated in our studies (Davids, 2020; Davids et al., (2021)). The presence of these phytochemicals has the ability to reduce bulk metals into their NPs form. Also, an earlier study by Islam et al. (2019) reported the synthesis and biological activity of AuNPs of 20-200 nm size from the gall extract of *Pistacia integerrima*, revealing the presence of amines, amides, and alcohol in the plant extract, which acted as capping and reducing agents. *Parkia biglobosa* leaves extract was used as a reducing and capping agent in this study to successfully reduce H₂AuCl₄ to AuNPs. After 30 minutes at room temperature, the solution's colour changed from light yellow to dark purple, indicating the formation of AuNPs. However, Azam et al. (2018) discovered a colour change after 20 minutes, which could be attributed to the use of an incubator, which may have facilitated a faster reduction reaction. The primary step in the biosynthesis of AuNPs is the characterization of important properties such as shape, size, stability, surface area, and dispersion (Ahmed & Ikram, 2016).

The UV-Vis absorption spectrum of the biosynthesized AuNPs revealed visible absorption bands, indicating the formation of AuNPs by *Parkia biglobosa* leaves, which is consistent with previous research studies (Davids, 2020; Davids et al., (2021)). The absorption band exhibits a

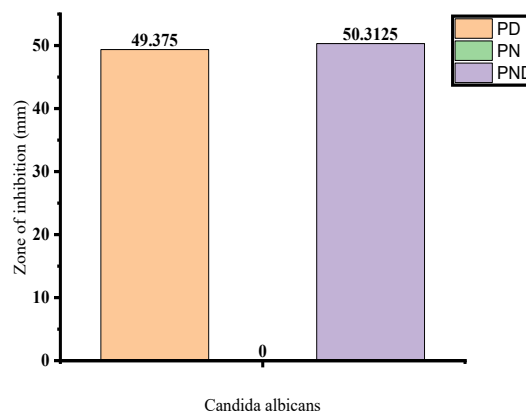


Figure 7: A graphic representation of anti-fungal potency of the nanodrugs against *Candida albicans* where P.N recorded no anti-fungal activities.

strong band at 530 nm, as well as an absorption band toward the NIR region Fig.2 (a). This red shift in the position of maximum absorption between H₂AuCl₄ and biosynthesized AuNPs indicates that *Parkia biglobosa* leaves have interacted with H₂AuCl₄, confirming successful AuNP synthesis (Davids, 2020; Davids et al., 2021; Azam et al., 2018; Sujitha & Kannan, 2013). From the TEM imaging studies, the average diameter of the biosynthesized AuNPs were around 2.04 ± 0.50 nm (fig. 2 (b)). It could be seen that, the sizes of the biosynthesized AuNPs are almost inconsistent with the already existing AuNPs. The TEM image shows that biosynthesized AuNPs have various morphologies mostly spherical in shape and less triangle, pentagon sphere, oval, truncated rod, and hexagon shapes, and high mono-dispersity. Additionally, the UV-Vis absorption spectra seen in Fig. 4 (a) confirms a successful formulation of the nanodrugs (PD, PN, PND). FTIR in Fig. 3 exhibited bands at 605.54 Cm⁻¹, 1074.16 Cm⁻¹, 1132.01 Cm⁻¹, 1274.72 Cm⁻¹, 1400.07 Cm⁻¹, 1625.70 Cm⁻¹, 2923.60 Cm⁻¹ and 3390.25 Cm⁻¹. The transmittance at 3390.25 Cm⁻¹ and 2923.60 Cm⁻¹ correspond to O-H stretching vibrations of phenol group and C-H stretching of aromatic compounds were observed respectively. Vibrations stretch at 1625.70 Cm⁻¹ attributes to C-C stretch of aromatic ring, confirming the presence of aromatic group. The characteristic band of primary amine group (-NH₂) can be assigned at 1400.00 cm⁻¹ for AuNPs (Noruzi et al., 2011; Rajan et al., 2017). The bonds related to N-H and aliphatic C-H represented the presence of proteins on the surface of the AuNPs. The presence of proteins on

the surface of NPs has been hypothesized to prevent agglomeration of the AuNPs (Narayanan & Sakhivel, 2011; Ajita et al., 2014). X-ray diffraction (XRD) was used to investigate the crystal structure of the biosynthesized AuNPs and compare their activity to that of standard Au. The XRD of *Parkia biglobosa* mediated AuNPs revealed Au peaks ranging from 30 to 80 at 2 degrees, as shown in Fig. 3 (b). The 38.197° diffraction peak is very intense, with slightly shifted and depressed peaks at 44.084°, 65.057°, and 78.055°. The Bragg's reflections for these peaks are (111), (200), (220), and (311), respectively (Davids, 2020; Davids et al., 2021). This corresponds to JCPDS card number 04-0784, which indicates face-centered cubic AuNPs with space group Fm-3 m (225). The (111) peak has a much higher intensity than the other peaks, indicating that the Au (111) plane is the dominant crystal facet in the synthesized Au nanoparticles. The presence of gold nanoparticles was revealed by EDS analysis of the AuNPs, as shown in Fig. 3 (a), where the horizontal axis represents the energy used in KeV and the vertical axis represents the number of counts. Carbon signals at 0.4 KeV, copper at 1.0 KeV, and silicon at 1.8 KeV stood out, with the highest peak revealed at around 2.20 KeV. It is worth noting that Au has more peaks than the other elements, indicating that the gold salt has been reduced, with the peaks at binding energies of 100, 8.0, and 9 representing copper and the first peak representing carbon (Davids, 2020).

Drug Release and Anti-microbial Efficiency

Drug Release

NPs have emerged as promising in the pharmaceutical industry, prompting several studies into their potential as drug delivery agents. The biocompatibility of NPs with cellular structures, bio-distribution properties, and easily tunable surface for functionalization all contribute to their potential for drug delivery in vivo. Antibiotic resistance has increased over time, as has the unrealistic bio-distribution of antibiotics to disease sites, making it critical to improve antibiotic efficiency in order to cure disease. From this study, the drug release efficiency of three formulated drugs based on PEG conjugated on lincomycin (PD), PEG conjugated on AuNPs (PN), and functionalization of AuNPs with both PEG and lincomycin (PND) has proven to be prudent in augmenting unrealistic bio-distribution and provide a new generation technology to curb microbial growth resistance against antibiotics. From Fig. 4 (b) it can be ascertained that the three (3) formulated drugs PD, PN and PND were released at 3 minutes but the highest peak was recorded in the drug which contains the 3 composite (PND) where its release capacity was 23mg / ml whereas both PD and PN record-

ed drug release capacity at 12mg/ ml and 4.8mg/ ml respectively at 9 minutes. The release activity seen with the PND drug composite could be a result of the combined interaction of both the PEG and AuNPs which averted the drug from early degradation, thereby sustaining the drug to elicit its activity which is in consonance with the earlier study by Shittu et al. (2017). The 4.8mg/ ml release capacity of the PN confirms the potential biocompatibility and long circulation time of NPs when functionalized with polymer such as PEG. So loading such a NP with a drug would be prudent for site target delivery without cellular accumulation.

Antimicrobial Studies

Antibiotic resistance is the ability of bacteria and other microbes to resist the effect of an antibiotic. This is because the bacteria alter themselves in a way that reduces or eradicates the effectiveness of drugs that are formulated to prevent their infection. The formulated drug composites were tested on 4 strains of bacteria namely; *Escherichia coli*, *Staphylococcus aureus*, *Enterococcus faecalis* and *Pseudomonas aeruginosa* and it was noted that the formulation which included the 3 composites (PND) had the greatest inhibition rate against all the four strains followed by (PD) while PN did not record any antibacterial inhibition ration as shown in Fig. 5. Additionally, Fig. 5 shows the anti-fungal potency of the three (3) formulated drugs and it was determined that the drug composed of the 3 composites (PND) registered the largest anti-fungal efficacy levels 50.313 % and the PD recorded 49.375% while the PN recorded no anti-fungal activity. Antibiotics coupled with inorganic nanoparticles have higher antibacterial properties. If the bacteria or pathogenic fungi are resistant to antibiotics, they may be killed by metal nanoparticles without influencing the biocompatibility of antibiotics (Siddiqi & Husen, 2017). Gu et al. (2003) have shown enhanced activity of vancomycin coated gold nanoparticles on vancomycin resistant enterococci. AuNPs coated with poly(ethyleneimine) for their biomedical application was studied for their antimicrobial activities. It is very encouraging to note that such gold nanoparticles retain their activity under most acidic and most basic conditions (pH 3 - pH 10) and inhibit growth of *Escherichia coli* and *Staphylococcus aureus* (Aslam et al., 2004). They inhibit the synthesis of peptidoglycan layer producing hole in bacterial cell wall, resulting in the leakage of cell material leading to their death which corresponds to our present study.

The highest inhibition was however observed in the fungus *C. albicans* with PND 50.3mm. A fundamental prerequisite for growth of *Candida* is regulation of its

pH and a mechanism to maintain this is by the activation of plasma membrane ATPase. According to Wani and Ahmad, the effect of AuNPs on *Candida* sp. is spontaneous and irreversible (Wani & Ahmad, 2013). Their study suggests that the interaction of AuNPs with transmembrane proteins such as ATPase alters the normal proton pump activity of the fungal cells leading to retardation of growth and finally cell death. [The antifungal activity of AuNPs is comparable to that reported for AuNPs synthesized using *A. esculentus*.

CONCLUSION

This study has demonstrated the bio-reduction and stability potential of bulk HAuCl₄ by the leaves of *Parkia biglobosa* due to the presence of their intrinsic phytochemicals. For the first time, *Parkia biglobosa* leaves mediated AuNPs was functionalized with a polymer, PEG and a standard antibiotic drug, lincomycin. Three different drug composites were formulated thus, PD (PEG conjugated on lincomycin), PN (PEG conjugated on AuNPs), and PND (PEG and lincomycin conjugated on AuNPs). To curb the growing menace of microbial drug resistance, unrealistic drug delivery, the as-synthesized drug composites were explored for their drug release efficiency with time and antimicrobial activities against some selected clinical isolates. At a initial drug release capacity of 3 minutes, an optimal released capacity was reached at 9 minutes for all three drugs composites (PD, PN, PND). Interestingly, the formulated drug comprising of PEG, drug (lincomycin), and AuNPs (PND) had the highest drug release capacity of 23mg/ ml followed by PD and PN of 12mg/ ml and 4.8ml respectively. We hypothesized that, the highest drug release capacity seen in the PND composite is due to the biocompatibility property of the AuNPs and the ability of PEG to prevent degradation of the AuNPs. The antimicrobial activity of the formulated drug composites were able to inhibit the growth of the microbes with PND inhibiting the growth of *Pseudomonas aeruginosa*, *Enterococcus faecalis*, *Staphylococcus aureus*, and *Escherichia coli* at 43.25 mm, 20.25 mm, 33.0 mm, and 28.00 mm, respectively, followed by PD on *Pseudomonas aeruginosa*, *Enterococcus faecalis*, *Staphylococcus aureus*, and *Escherichia coli* with the zones of inhibition at 41.75 mm, 19 mm, 30.75 mm, and 23.5 mm, respectively. PND and PD both inhibited *Candida albicans* with zones of inhibition of 50.31 mm and 49.34 mm, respectively. The combined drug release potential and microbial growth inhibition of the as-synthesized formulated drugs provide a new generation technology to improve

disease treatment capacity of pharmaceutical drugs as such drugs will have extended blood circulation, and serum adsorption escape.

References

- Agarwal, H., Kumar, S. V., & Rajeshkumar, S. (2017). A review on green synthesis of zinc oxide nanoparticles—An eco-friendly approach. *Resource-Efficient Technologies*, 3(4), 406-413. doi:<https://doi.org/10.1016/j.reffit.2017.03.002>
- Ahmed, S., & Ikram, S. (2016). Biosynthesis of gold nanoparticles: a green approach. *Journal of Photochemistry and Photobiology B: Biology*, 161, 141-153.
- Ajitha, B., Reddy, Y. A. K., & Reddy, P. S. (2014). Biogenic nano-scale silver particles by *Tephrosia purpurea* leaf extract and their inborn antimicrobial activity. *Spectrochimica Acta Part A: Molecular and Biomolecular Spectroscopy*, 121, 164-172.
- Akinyemi, K. O., Oladapo, O., Okwara, C. E., Ibe, C. C., & Fasure, K. A. (2005). Screening of crude extracts of six medicinal plants used in South-West Nigerian unorthodox medicine for anti-methicillin resistant *Staphylococcus aureus* activity. *BMC complementary alternative medicine*, 5(1), 1-7.
- Andra, S., Balu, S. K., Jeevanandham, J., Muthalagu, M., Vidyavathy, M., Chan, Y. S., & Danquah, M. K. (2019). Phytosynthesized metal oxide nanoparticles for pharmaceutical applications. *Naunyn-Schmiedeberg's archives of pharmacology*, 392(7), 755-771.
- Aslam, M., Fu, L., Su, M., Vijayamohan, K., & Dravid, V. P. (2004). Novel one-step synthesis of amine-stabilized aqueous colloidal gold nanoparticles. *Journal of materials Chemistry*, 14(12), 1795-1797.
- Bhardwaj, B., Singh, P., Kumar, A., Kumar, S., & Budhwar, V. (2020). Eco-friendly greener synthesis of nanoparticles. *Advanced Pharmaceutical Bulletin*, 10(4), 566. doi:<https://doi.org/10.34172/apb.2020.067>
- Chahardoli, A., Karimi, N., Sadeghi, F., & Fattahi, A. (2018). Green approach for synthesis of gold nanoparticles from *Nigella arvensis* leaf extract and evaluation of their antibacterial, antioxidant, cytotoxicity and catalytic activities. *Artificial cells, nanomedicine, and biotechnology*, 46(3), 579-588.
- Chakraborty, N., Gandhi, S., Verma, R., & Roy, I. (2022). Emerging prospects of nanozymes for antibacterial and anticancer applications. *Biomedicine*, 10(6), 1378.
- Chen, J., Wang, H., Long, W., Shen, X., Wu, D., Song, S.-S., Sun, Y.-M., Liu, P.-X., Fan, S., & Zhang, X.-D. (2013). Sex differences in the toxicity of polyethylene glycol-coated gold nanoparticles in mice. *Inter-*

- national journal of nanomedicine*, 8, 2409. doi:10.2147/FIJN.S46376
- Davids, J. S., Ackah, M., Okoampah, E., Fometu, S. S., Guohua, W., & Jianping, Z. (2021) Biocontrol of Bacteria Associated with Pine Wilt Nematode, *Bursaphelenchus xylophilus* by using Plant mediated Gold Nanoparticles. *International Journal of Agriculture & Biology*, 26(4). doi:10.17957/IJAB/15.1863
- Del Pino, P., Yang, F., Pelaz, B., et al. (2016). Basic physicochemical properties of polyethylene glycol coated gold nanoparticles that determine their interaction with cells. *Angewandte Chemie*, 128(18), 5573-5577.
- Gajdács, M., Urbán, E., Stájer, A., & Baráth, Z. (2021). Antimicrobial resistance in the context of the sustainable development goals: A brief review. *European Journal of Investigation in Health, Psychology Education*, 11 (1), 71-82.
- Gu, H., Ho, P., Tong, E., Wang, L., & Xu, B. (2003). Presenting vancomycin on nanoparticles to enhance antimicrobial activities. *Nano letters*, 3(9), 1261-1263.
- Howden-Chapman, P., Siri, J., Chisholm, E., Chapman, R., Doll, C. N., & Capon, A. (2017). SDG 3: Ensure healthy lives and promote wellbeing for all at all ages. *A guide to SDG interactions: from science to implementation. Paris, France: International Council for Science*, 81-126.
- Islam, N. U., Jalil, K., Shahid, M., Muhammad, N., & Rauf, A. (2019). Pistacia integerrima gall extract mediated green synthesis of gold nanoparticles and their biological activities. *Arabian Journal of Chemistry*, 12(8), 2310-2319.
- Jayaseelan, C., Ramkumar, R., Rahuman, A. A., & Perumal, P. (2013). Green synthesis of gold nanoparticles using seed aqueous extract of *Abelmoschus esculentus* and its antifungal activity. *Industrial Crops and Products*, 45, 423-429.
- Kale, S. K., Parishwad, G. V., Patil, A. S. H. A. S., & Agroforestry. (2021). Emerging agriculture applications of silver nanoparticles. *ES Food & Agroforestry*, 3, 17-22.
- Kaur, K., & Sidhu, A. K. (2021). Green synthesis: An eco-friendly route for the synthesis of iron oxide nanoparticles. *Frontiers in Nanotechnology*, 3, 47. doi:<https://doi.org/10.3389/fnano.2021.655062>
- Kazmi, S. A. R., Qureshi, M. Z., Ali, S., & Masson, J. F. (2019). In Vitro Drug Release and Biocatalysis from pH-Responsive Gold Nanoparticles Synthesized Using Doxycycline. *Langmuir*, 35(49), 16266-16274. doi:10.1021/acs.langmuir.9b02420
- Khan, K., Tareen, A. K., Iqbal, M., Wang, L., Ma, C., Shi, Z., . . . Shams, S. S. (2021). Navigating recent advances in mono-elemental materials (Xenes)-fundamental to biomedical applications. *Progress in Solid State Chemistry*, 63, 100326.
- Koperuncholan, M. (2015). Bioreduction of chloroauric acid (HAuCl₄) for the synthesis of gold nanoparticles (GNPs): A special emphasis of pharmacological activity. *Int. J. Phytopharm*, 5(4), 72-80.
- Lin, Z., Monteiro-Riviere, N. A., & Riviere, J. E. (2016). A physiologically based pharmacokinetic model for polyethylene glycol-coated gold nanoparticles of different sizes in adult mice. *Nanotoxicology*, 2016. 10 (2), 162-172.
- Narayanan, K. B., & Sakthivel, N. (2011). Green synthesis of biogenic metal nanoparticles by terrestrial and aquatic phototrophic and heterotrophic eukaryotes and biocompatible agents. *Advances in colloid and interface science*, 169(2), 59-79.
- Noruzi, M., Zare, D., Khoshnevisan, K., & Davoodi, D. (2011). Rapid green synthesis of gold nanoparticles using *Rosa hybrida* petal extract at room temperature. *Spectrochimica Acta Part A: Molecular and Biomolecular Spectroscopy*, 79(5), 1461-1465.
- Okoampah, E., Mao, Y., Yang, S., Sun, S., & Zhou, C. (2020). Gold nanoparticles–biomembrane interactions: From fundamental to simulation. *Colloids and Surfaces B: Biointerfaces*, 196, 111312. doi:<https://doi.org/10.1016/j.colsurfb.2020.111312>
- World Health Organization. (2018). *Tackling antimicrobial resistance (AMR) together: working paper 5.0: enhancing the focus on gender and equity*. Retrieved from
- Rajan, A., Rajan, A. R., & Philip, D. (2017). Elettaria cardamomum seed mediated rapid synthesis of gold nanoparticles and its biological activities. *OpenNano*, 2, 1-8.
- Sardella, D., Gatt, R., & Valdramidis, V. P. (2018). Turbidimetric assessment of the growth of filamentous fungi and the antifungal activity of zinc oxide nanoparticles. *Journal of food protection*, 81(6), 934-941.
- Shine, D. J., Shasha, S., Emmanuel, O., Fometu, S. S., & Guohua, W. (2020). Biosynthesizing Gold Nanoparticles with *Parkia biglobosa* Leaf Extract for Antibacterial Efficacy In Vitro and Photocatalytic Degradation Activities of Rhodamine B Dye. *Advanced Science, Engineering Medicine*, 12(7), 970-981.
- Shittu, K., Bankole, M., Abdulkareem, A., Abubakre, O., & Ubaka, A. (2017). Application of gold nanoparticles for improved drug efficiency. *Advances in Natural Sciences: Nanoscience and Nanotechnology*, 8(3), 035014.
- Siddiqi, K. S., & Husen, A. (2017). Recent advances in plant-mediated engineered gold nanoparticles and their application in biological system. *Journal of Trace Elements in Medicine and Biology*, 40, 10-23.
- Singh, R., Patil, S., Singh, N., & Gupta, S. (2017). Dual

- functionality nanobioconjugates targeting intracellular bacteria in cancer cells with enhanced antimicrobial activity. *Sci Rep*, 7(1), 5792. doi:10.1038/s41598-017-06014-4
- Singh, S., Kumar, V., Romero, R., Sharma, K., & Singh, J. (2019). Applications of nanoparticles in wastewater treatment. In *Nanobiotechnology in bioformulations* (pp. 395-418): Springer.
- Sujitha, M. V., & Kannan, S. (2013). Green synthesis of gold nanoparticles using Citrus fruits (Citrus limon, Citrus reticulata and Citrus sinensis) aqueous extract and its characterization. *Spectrochimica Acta Part A: Molecular and Biomolecular Spectroscopy*, 102, 15-23.
- Wani, I. A., & Ahmad, T. (2013). Size and shape dependant antifungal activity of gold nanoparticles: a case study of Candida. *Colloids and Surfaces B: Biointerfaces*, 101, 162-170.
- Zhang, Z., Jia, J., Lai, Y., Ma, Y., Weng, J., & Sun, L. (2010). Conjugating folic acid to gold nanoparticles through glutathione for targeting and detecting cancer cells. *Bioorg Med Chem*, 18(15), 5528-5534.